

滑动轴承支撑转子系统混沌响应计算

武新华¹, 张新江¹, 于增波²

(1. 哈尔滨工业大学 能源学院, 黑龙江 哈尔滨 150001; 2. 哈尔滨汽轮机厂, 黑龙江 哈尔滨 150040)

摘要:以转子动力学和非线性动力学理论为基础, 针对非线性转子—轴承系统的具体特点, 建立了采用短轴承模型的弹性转子—轴承系统模型, 并用数值积分和庞加莱映射方法对其在某些参数域中进行了非线性振动研究, 得到了系统在某些参数域中的分叉图、庞加莱映射和随转速变化的三维谱图, 计算结果显示, 系统有可能发生混沌运动。对系统动力学特性随某些参数变化时的非线性特性进行了分析, 直观显示了参数变化对系统动力学特性的影响, 为该类转子—轴承系统的设计提供了理论参考。

关键词:叶轮机械; 转子动力学; 转子—轴承系统; 非线性振动; 混沌

中图分类号: TH133.3 文献标识码: A

1 引言

转子—轴承系统是叶轮机械的重要部件。其中, 在具有滑动轴承的转子系统中, 由于非线性油膜力的作用将使转子在某些参数域中产生相当大的振动, 因此, 分析该类系统的振动特性和稳定性一直是转子动力学研究中的重要课题。国内外许多文献对该类系统在刚性、无阻尼假设条件下进行了研究。陈子恕^[1]用快速 Galerkin 方法结合 Floquet 理论和数值方法, 对具有非线性油膜力的 Jeffcott 转子—轴承系统进行了分叉研究; J. W. Zu^[2]用谐波平衡法对该类系统的稳态响应进行了求解; S. Boedol^[3]则认为阶梯轴承比普通圆柱轴承性能优越; 刘恒^[4]用伪不动点追踪法将该类系统的周期解求解问题转化为标量函数的寻优问题进行求解。但对弹性转子—轴承系统的论述很少。

针对上述情况, 为更接近实际转子运行状况, 本文主要研究一个具有非线性油膜力的弹性转子—轴承系统的非线性动力学问题。基础刚度采用非线性刚度假设^[5], 用数值算法得到了系统的分叉图及三维谱图, 直观显示了系统的运动状态和特点。庞加莱映射及频谱也表明系统具有发生混沌运动的可

能, 同时对参数变化对系统动力学特性的影响进行了分析, 为采用该类轴承的转子—轴承系统的设计提供理论参数。

2 数学模型

非线性弹性转子—轴承—基础系统的数学模型如图1所示。

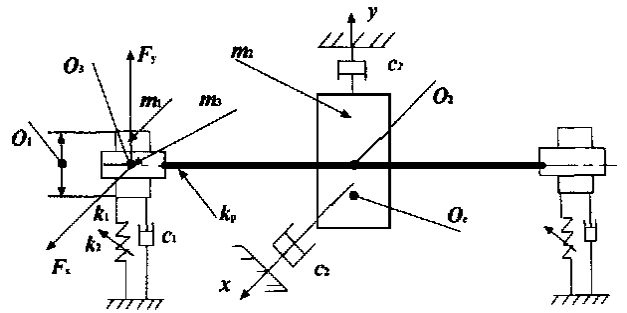


图1 弹性转子—轴承系统
 o_1 —轴承中心; m_1 —轴承质量, k_1, k_2 —轴承支撑结构刚度;
 c_1 —轴承支撑结构阻尼; $2k_v$ —转轴刚度; F_x, F_y —非线性油膜力分量; o_2 —转子几何中心; o_3 —转子质心; m_2 —转子圆盘质量;
 c_2 —转子圆盘阻尼; o_3 —转轴中心; m_3 —转轴集中质量。

图1 弹性转子—轴承系统

在转子角速度为 ω , 无量纲偏心为 $\rho = e/c$ 时, 系统在对称性假设条件下的无量纲微分方程为:

$$\begin{cases} \ddot{x}_1 = -\frac{a_1}{m_1}x_1 - \frac{a_2}{m_1}x_1 - \frac{a_3}{m_1}x_1^3 + \frac{1}{m_{11}}f_x \\ \ddot{y}_1 = -\frac{a_1}{m_1}y_1 - \frac{a_2}{m_1}y_1 - \frac{a_3}{m_1}y_1^3 + \frac{1}{m_{11}}f_y - G \\ \ddot{x}_2 = -\frac{a_5}{m_2}x_2 - \frac{2a_4}{m_2}(x_2 - x_3) + \rho \cos\tau \\ \ddot{y}_2 = -\frac{a_5}{m_2}y_2 - \frac{2a_4}{m_2}(y_2 - y_3) + \rho \sin\tau - G \\ \ddot{x}_3 = -\frac{a_6}{m_3}x_3 - \frac{a_4}{m_3}(x_3 - x_2) + \frac{1}{m_{31}}f_x \\ \ddot{y}_3 = -\frac{a_6}{m_3}y_3 - \frac{a_4}{m_3}(y_3 - y_2) + \frac{1}{m_{31}}f_y - G \end{cases} \quad (1)$$

收稿日期: 2000-03-20; 修订日期: 2000-05-16

基金项目: 国家自然科学基金资助(重大)项目(19990510)

作者简介: 张新江(1967—), 男, 山东招远人, 哈尔滨工业大学博士研究生。

其中,无量纲坐标 $x_i = X_i/c, y_i = Y_i/c, f_x = F_x/\delta, f_y = F_y/\delta$ —无量纲非线性油膜力分量; $\delta = \frac{\mu\omega RL}{m_3g} \left(\frac{R}{c}\right)^2 \left(\frac{L}{2R}\right)^2$ —Sommerfeld 修正数; μ —润滑油粘度; $G = \frac{g}{c\omega}$ —无量纲外载荷; $\tau = \omega t$ —无量纲时间; e —偏心量; c —轴承半径间隙, L —轴承长度, R —轴承半径; $m_{11} = m_1\omega^2c/s, m_{31} = m_3\omega^2c/\delta, a_1 = c_1/\omega, a_2 = k_1/\omega^2, a_3 = k_2\delta/\omega^2, a_4 = k_p/\omega^2, a_5 = c_2/\omega, a_6 = c_3/\omega, f_x, f_y$ 由文献 [6] 确定:

$$\begin{cases} f_x \\ f_y \end{cases} = - \frac{[(x-2y')^2 + (y+2x')^2]^{1/2}}{1-x^2-y^2} \times \begin{cases} 3xV(x, y, \alpha) - \sin\alpha G(x, y, \alpha) - 2\cos\alpha S(x, y, \alpha) \\ 3yV(x, y, \alpha) + \cos\alpha G(x, y, \alpha) - 2\sin\alpha S(x, y, \alpha) \end{cases}$$

式中, $x = x_3 - x_1, x' = (x_3 - x_1)', y = y_3 - y_1, y' = (y_3 - y_1)'$

$$V(x, y, \alpha) = \frac{2 + (y\cos\alpha - x\sin\alpha)G(x, y, \alpha)}{1 - x^2 - y^2},$$

$$S(x, y, \alpha) = \frac{x\cos\alpha + y\sin\alpha}{1 - (x\cos\alpha + y\sin\alpha)^2},$$

$$G(x, y, \alpha) = \frac{2}{(1 - x^2 - y^2)^{1/2}} \times \left[\frac{\pi}{2} + \arctg \frac{y\cos\alpha - x\sin\alpha}{(1 - x^2 - y^2)^{1/2}} \right],$$

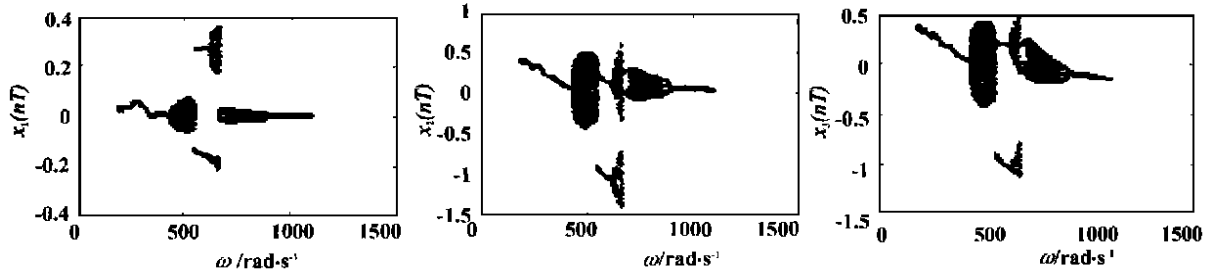


图 2 $e = 0.06 \text{ mm}$ 时 x_1, x_2, x_3 随 ω 变化的分叉图

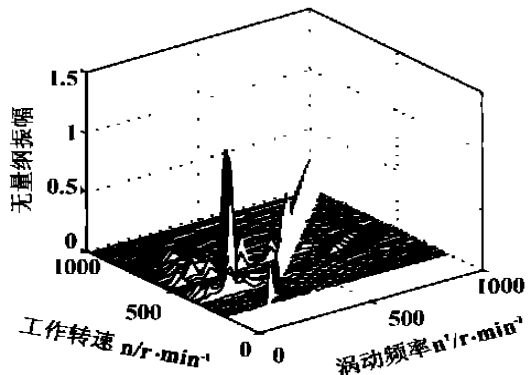


图 3 o_2 在 x 方向的三维谱图

$$\alpha = \arctg \frac{y + 2x'}{x - 2y'} - \frac{\pi}{2} \text{sign} \left(\frac{y + 2x'}{x - 2y'} \right) - \frac{\pi}{2} \text{sign}(y + 2x')$$

3 数值积分

由于油膜力的强非线性特征,因此选用龙格—库塔法。本文选用的时间步长为 $\pi/100$, 误差小于 0.001, 选用 Fortran90 编程, 所得数据用于分叉图及三维谱图。

3.1 分叉图

本文取 $m_1 = 98 \text{ kg}, m_2 = 420 \text{ kg}, m_3 = 50 \text{ kg}, D = 114 \text{ mm}, L = 28.5 \text{ mm}, c = 0.2 \text{ mm}, \mu = 18 \times 10^{-3} \text{ Pa} \cdot \text{s}, k_1 = 5.26 \times 10^6 \text{ N/m}, k_2 = 1.26 \times 10^{12} \text{ N/m}, k_p = 1.052 \times 10^8 \text{ N/m}, c_1 = 4.3 \times 10^5 \text{ N} \cdot \text{s/m}, c_2 = 3.3 \times 10^4 \text{ N} \cdot \text{s/m}, c_3 = 3.3 \times 10^4 \text{ N} \cdot \text{s/m}$, 通过跟踪数值积分中参变量 ω 及 ρ 值的变化, 从图 2 中观察 ω 的值在 $200 \sim 1100 \text{ rad/s}$ 之间变化时, 系统的运动规律。从图 3 中观察在定转速下 ρ 的变化范围为 $0.05 \sim 0.5$ 区域内位移 x_1, x_2, x_3 的不同性质, 可以发现转子系统的概周期运动及混沌解以及系统随偏心改变时的运动规律。

从图 2 中可以看出, 在一定偏心质量作用下, 转子—轴承系统随转速的增加, 经历了周期 \rightarrow 概周期 \rightarrow 倍周期 \rightarrow 四倍周期 \rightarrow 混沌 \rightarrow 倍周期 \rightarrow 周期运动。为更清晰地表现这一变化过程, 作者画出了 ω 在 $300 \sim 1100 \text{ rad/s}$ 之间变化时 o_2 在 x 方向的三维谱图, 如图 3 所示。当 $\omega = 720 \text{ rad/s}$ 时系统的三维谱图上出现连续谱, 表明系统可能发生了混沌运动。

3.2 其他结果

取 $e = 0.06 \text{ mm}, \omega = 720 \text{ rad/s}$ 时的 x_1, x_2, x_3 的庞加莱映射, 相图及频谱图, 如图 4 所示, 可以看到混沌运动状态的动力特性。图 4 显示, 庞加莱映射

具有几何分形结构, 表明系统发生了混沌运动。

4 几何参数对转子—轴承系统动力学特性的影响

取 $e = 0.06 \text{ mm}$, $\omega = 720 \text{ rad/s}$ 时的 x_1, x_2, x_3 随基础线性刚度 k_1 、非线性刚度 k_2 、基础阻尼 c_1 变化的分叉图如图 5 ~ 图 7 所示。

从图 5 ~ 图 7 可以看出, 随基础刚度和阻尼的增加, 系统由混沌运动变为稳定的周期运动。

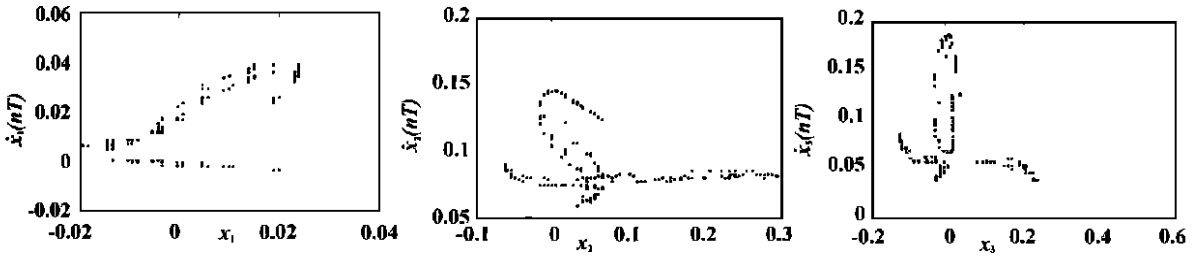


图 4 $\omega = 720 \text{ rad/s}$ 时的庞加莱映射特征曲线

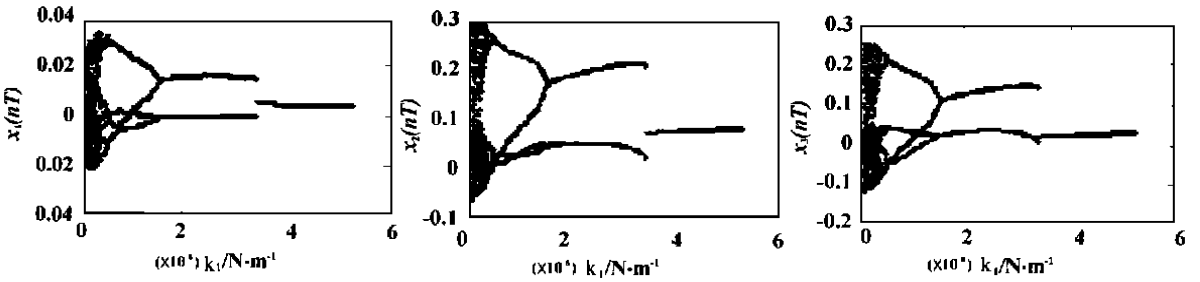


图 5 x_1, x_2, x_3 随 k_1 变化的分叉图

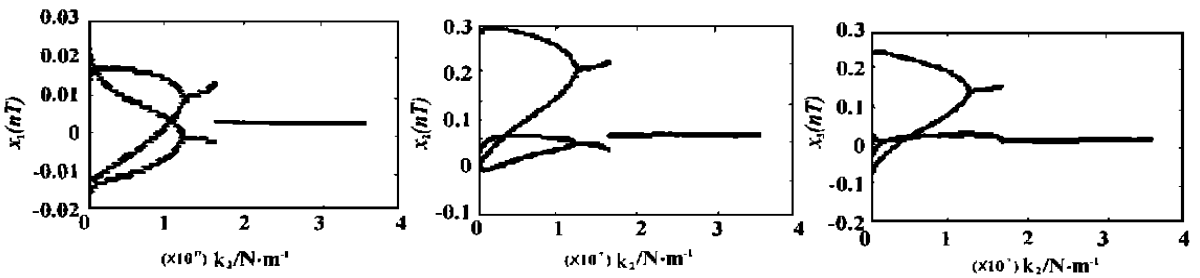


图 6 x_1, x_2, x_3 随 k_2 变化的分叉图

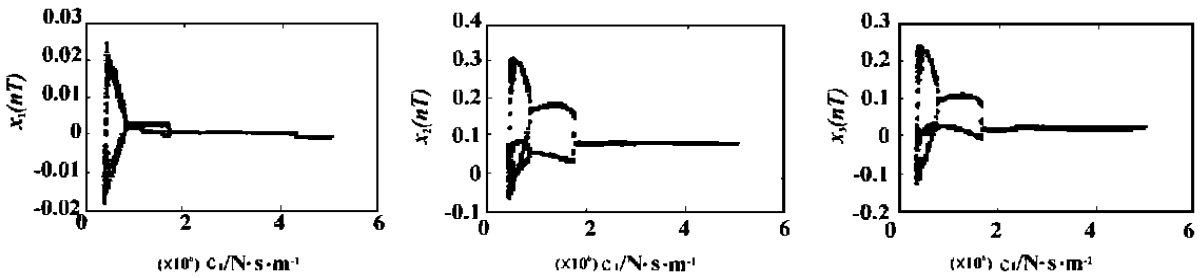


图 7 x_1, x_2, x_3 随 c_1 变化的分叉图

5 结 论

(1) 弹性转子—轴承系统在一定偏心质量作用下随转速的增加具有产生混沌运动的能力,混沌运动容易引起转子—轴承系统产生疲劳破坏并可能导致系统失稳,因此在设计过程中应避免该区域。

(2) 偏心质量和非线性油膜力是导致混沌运动的根本原因,倍周期运动是通向混沌的道路。数值计算结果表明,该类转子—轴承系统在四倍周期分叉后产生混沌运动。

(3) 在一定偏心质量下,该类系统运动状态随转速的升高超过某一值后混沌运动消失。

(4) 改变基础参数可以有效避开混沌运动区域,计算结果表明,增加基础刚度、阻尼,可以消除混沌运动,保证系统安全运行。

上述结论可以为该类转子—轴承系统的设计和

安全运行提供定性参数。

参考文献:

- [1] 陈予恕,孟泉.非线性转子—轴承系统的分叉[J].振动工程学报,1996,9(3):266—275.
- [2] ZU J W,JI Z Y. Steady-state response of continuous nonlinear rotor-bearing systems using analytical approach[J]. *ASME Journal of Engineer for Gas Turbines and Power*, 1998, **120**:751—758.
- [3] BOEDO S. Global stability analysis of cylindrical and dual offset rotor bearing system[J]. *Nonlinear Dynamics* 1998, **16**:187—202.
- [4] 刘恒,虞烈,谢友柏.非线性动力系统多重周期解的伪不动点追踪法[J].力学学报,1999,31(2):222—229.
- [5] CHEN Chieh-li, YAN Her-Teng. Chaos in the imbalance response of a flexible rotor supported by oil film bearing with nonlinear suspension [J]. *Nonlinear Dynamics*, 1998, **16**:71—90.
- [6] ADILETTA G, GUIDO A R, ROSSI C. Chaotic motions of a rigid rotor in short journal bearings[J]. *Nonlinear Dynamics*, 1996 **10**:251—269.

(复 编辑)

(上接第 370 页)

(2) 加压对城市生活垃圾典型有机组份裂解初始时间、持续时间和失重率的影响:

(a) 随压力升高,裂解初始温度升高,达到一定压力后,当压力进一步升高时,裂解初始温度反而下降。

(b) 随压力升高,裂解初始时间后移,但随压力进一步升高时,裂解初始时间反而前移。

(c) 随压力升高,对不同物料的裂解持续时间有不同的影响,可能加快也可能减慢。

(d) 随压力升高,裂解失重率下降。

(3) 由五种 RDF 典型有机组份加压热解试验数据及动力学模型得出其热解反应可视为一级反应,即 $d\alpha/dt = A[\exp(-E/RT)](1-\alpha)$ 。

参考文献:

- [1] SHUGO HOSODA, NOBUTAKA KASHIMA, SHINJI SEIKAWA. Status of pressurized internally circulating fluidized-bed gasifier (PICFG) development project [A], Proceedings of the 15th International Conference on Fluidized Bed Combustion [C]. Savannah, Georgia ASME, 1999:16—19.

- [2] JIN Bao-sheng, ZHONG Zhao-ping, ZHOU Shan-ming. Fundamental study on pyrolysis of municipal solid wastes (MSW)[J], *Developments in Chemical Engineering and Mineral Processing*, 1999, **7** (5):611—622.
- [3] COLETTE Braekman-Danheux. Upgrading of waste derived solid fuel by steam gasification[J]. *Fuel*, 1998 **77**(1/2):55—59.
- [4] COATS A W, REDFERN J P. Kinetic parameters from thermogravimetric data [J]. *Nature* 1964, **68**:201.
- [5] COZZANIL V. A fundamental study on conventional pyrolysis of a Refuse Derived Fuel[J]. *Ind Eng Chem Res*, 1995 (34):2006—2020.
- [6] ANTAL M J, VARHEGYIN G. Cellulose pyrolysis kinetics: the current state of knowledge [J]. *Ind Eng Chem Res* 1995 (34):707—717.
- [7] 金保升,仲兆平,周山明.城市生活垃圾热分解特性的试验研究[J].环境工程,1998, **16**(6):51—55.
- [8] 章名耀,金保升.增压流化床联合循环发电技术[M].南京:东南大学出版社,1998:1—25.
- [9] 江淑琴.城市生活垃圾的燃烧性能研究[A].中国工程热物理学会燃烧学学术会议[C].天津:中国工程热物理学会,1997:7:26—33.
- [10] 屈超蜀,唐炜柏,代贵.城市生活垃圾处理工程[M].重庆:重庆大学出版社,1994:90—98.

(复 编辑)

presented is a relevant pyrolysis mechanism. **Key words:** refuse derived fuel, pyrolysis characteristics, kinetic parameter, thermogravimetric analysis

滑动轴承支撑转子系统混沌响应计算 = **The Calculation of Chaotic Response of a Journal Bearing-supported Rotor System** [刊, 汉] / WU Xin-hua, ZHANG Xin-jiang (Energy College under the Harbin Institute of Technology, Harbin, China, Post Code: 150001), YU Zeng-bo (Harbin Turbine Works, Harbin, China, Post Code: 150046) // Journal of Engineering for Thermal Energy & Power. — 2001, 16(4). — 371 ~ 374

On the basis of the theory of rotor dynamics and nonlinear dynamics and in the light of the specific features of a nonlinear rotor-bearing system set up was a model of elastic rotor-bearing system with the use of a short bearing model. Moreover, through the use of a numerical integration and Poincaré mapping method a nonlinear vibration study was conducted of the above rotor-bearing system in the domain of certain parameters. As a result, obtained for the system in the above domain were bifurcation diagrams, Poincaré mappings and speed-varied three-dimensional spectral diagram. The results of calculation indicate that the rotor-bearing system may be subject to chaotic motions. An analysis was conducted of the nonlinear behavior of the system dynamics characteristics, which may vary with the change of certain parameters. A visual display is thereby obtained of the influence of parameter variation on the system dynamics characteristics. The above work can provide some theoretical reference data for the design of elastic rotor-bearing systems. **Key words:** turbomachinery, rotor dynamics, rotor-bearing system, nonlinear vibration, chaotic response

分离式热管换热器的工作原理及其在电厂余热回收中的应用 = **Working Principle of a Separation-type Heat-Pipe Heat Exchanger and Its Use in the Heat Recovery System of a Power Plant** [刊, 汉] / LIU Xiao-zhou, HUI Shi-en, XU Tong-mo, et al (Boiler Research Institute under the Xi'an Jiaotong University, Xi'an, Shaanxi Province, China, Post Code: 710049) // Journal of Engineering for Thermal Energy & Power. — 2001, 16(4). — 375 ~ 376, 379

Described is the working principle of a separation-type heat-pipe heat exchanger along with its use in a separation-type heat-pipe economizer installed on a 670 t/h boiler of a 200 MW power plant. A comparison of the above-cited heat exchanger with a conventional low-pressure economizer shows that the recommended heat exchanger enjoys tremendous superiority in terms of heat recovery efficiency. **Key words:** separation type heat pipe, working principle, low-pressure economizer, economic benefit

水平管内油气水三相间歇流向环状流转换的研究 = **An Investigation on the Intermittent-to-Annular Flow Transition of Oil-gas-water Three-phase Flow in a Horizontal Tube** [刊, 汉] / ZHOU Yun-long, CAI Hui, HONG Wen-peng, LI Yan (Power Engineering Department, Northeastern Electric Power Institute, Jilin, China, Post Code: 132012) // Journal of Engineering for Thermal Energy & Power. — 2001, 16(4). — 377 ~ 379

An experimental and theoretical study was conducted of the intermittent-to-annular flow transition of oil-gas-water three-phase flow in a horizontal tube. Proposed was a boundary equation featuring the transition of the intermittent-to-annular flow. The experimental study results show that the major factor governing the transition of the intermittent-to-annular flow is the gas-phase reduced speed and the liquid-phase reduced one with the effect of oil fraction and tube diameter playing an insignificant role. The results of calculation have been found to be basically in agreement with those of experiment. **Key words:** horizontal tube, oil-gas-water three-phase flow, flow pattern transition.

火床炉室内横向配风特性的理论分析 = **Theoretical Analysis of the Characteristics of Air Transverse Flow Distribution in a Stoker-boiler Air Compartment** [刊, 汉] / MIAO Zheng-qing, DOU Wen-yu, ZHOU Qu-lan, et al (Power and Energy College under the Xi'an Jiaotong University, Xi'an, China, Post Code: 710049) // Journal of Engineering for Thermal Energy & Power. — 2001, 16(4). — 380 ~ 382

Presented is an enclosed set of equations, which describes the air flow in a flow stabilized section of a stoker boiler dual lateral-side full-section air feed compartment and a full lateral-side air feed compartment. Through a theoretical deduction obtained was an analytical solution along with the deduction of a theoretical expression of the stoker surface flow-rate deviation. On this basis the limiting flow rate deviation location and the flow rate deviation limiting ratio were compared for the following cases: the dual lateral-side air feed mode and the single lateral-side air feed mode. Moreover, an analysis was performed of influence of air compartment construction and stoker grate layer structure on the flow rate deviation. **Key words:** stoker boiler, stoker air compartment, flow characteristics, flow distribution, flow deviation